Effect of Electron Donors on the Radical Polymerization of Vinyl Acetate Mediated by [Co(acac)2]: Degenerative Transfer versus Reversible Homolytic Cleavage of an Organocobalt(III) Complex

Sébastien Maria, Hiromu Kaneyoshi, Krzysztof Matyjaszewski, Rinaldo Poli

Effect of Electron Donors on the Radical Polymerization of Vinyl Acetate Mediated by [Co(acac)]$_2$: degenerative transfer versus reversible homolytic cleavage of an organocobalt(III) complex

Sébastien Maria,[a] Hiromu Kaneyoshi,[b] Krzysztof Matyjaszewski,[*b] and Rinaldo Poli[*a]

[a]*Laboratoire de Chimie de Coordination, UPR CNRS 8241 liée par convention à l'Université Paul Sabatier et à l'Institut National Polytechnique de Toulouse, 205 Route de Narbonne, 31077 Toulouse Cedex, France*

[b]*Center for Macromolecular Engineering, Department of Chemistry, Carnegie Mellon University, 4400 Fifth Avenue, Pittsburgh, Pennsylvania 15213*

*Corresponding authors. E-mail: poli@lcc-toulouse.fr

Abstract

The molecular structure of bis(acetylacetonate)cobalt(II) ($Co(acac)_2$) in solution and in the presence of the electron donors (ED) pyridine (py), NEt_3 and vinyl acetate (VOAc) was investigated using ^1H NMR spectroscopy in C_6D_6. The extent of formation of ligand adducts, $Co(acac)_2(ED)_x$, varies in the order py > NEt_3 > VOAc (no interaction). Density functional theory (DFT) calculations on model system agree with Co-ED bond strengths decreasing in the same order. The effect of electron donors on the $Co(acac)_2$-mediated radical polymerization of VOAc was examined at 30 ^oC by the addition of excess py or NEt_3 to the complex in the following molar ratio ($[VOAc]_0/[Co]_0/[V\text{-}70]_0/[py\ or\ NEt_3]_0$=500/1/1/30). Whereas, as previously reported (A. Debuigne, J.-R. Caille, R. Jerome, *Angew. Chem. Int. Ed.* **2005**, *44*, 1101.), the polymerization showed long induction periods in the absence of ED, a controlled polymerization process, though the level of control was poorer, took place without induction period in the presence of ED. The effective polymerization rate decreased in the order py > NEt_3. A similar behavior was found when these electron donors were added to an ongoing $Co(acac)_2$-mediated radical polymerization of VOAc. On the basis of the NMR and DFT studies, it is proposed that the polymerization is controlled by the reversible homolytic cleavage of an organocobalt(III) dormant species in the presence of ED. Conversely, the faster polymerization after the induction period in the absence of ED is due to a degenerative transfer process with the radicals produced by the continuous decomposition of the excess initiator. Complementary experiments provide additional results in agreement with this interpretation.

Keywords Controlled radical polymerization, organometallic, homolytic bond cleavage,

degenerative transfer, cobalt coordination chemistry, DFT calculations

Introduction

Recent progress in controlled radical polymerization (CRP)[1] processes allows the synthesis of various well-defined polymer structures in a controlled fashion. Three different CRP mechanisms have been extensively investigated (Scheme 1).[2] The first mechanism (eq. 1) is based on a spontaneous reversible homolytic cleavage of a dormant chain end and is exemplified by nitroxide-mediated polymerization (NMP)[3] or organometallic radical polymerization (OMRP).[4] The second process (eq. 2) involves a catalytic reversible homolytic cleavage of a carbon-halogen bond via a redox process, which occurs in atom transfer radical polymerization (ATRP).[5] The third one (eq. 3) is based on a thermodynamically neutral bimolecular exchange between propagating radicals and a dormant species. Degenerative transfer (DT) polymerization with alkyl iodides,[6] organotellurium or organostibine species[7] belongs in this category as well as reversible addition-fragmentation chain transfer (RAFT)[8] polymerization and macromolecular architecture design by interchange of xanthates (MADIX).[9] Recently, organocobalt compounds have been shown to provide the controlled polymerization of acrylates, acrylic acid and vinyl acetate by this degenerative transfer mechanism.[10]

Insert Scheme 1

One of the most promising CRP processes for conducting a successful controlled polymerization of VOAc is the recently reported $Co(acac)_2$-mediated polymerization.[4e, 4f] This was initiated with 2,2'-azobis(4-methoxy-2,4-dimethylvaleronitrile) (V-70) in the

presence of bis(acetylacetonate)cobalt(II) ($Co(acac)_2$), resulting in the formation of poly(vinyl acetate) (PVOAc) with predetermined M_n and low polydispersity. This system has been proposed to follow the OMRP mechanism (Scheme 1, equation 1 with X = $Co(acac)_2$). There is, however, an important feature of this efficient polymerization system that needs clarification. It concerns the puzzling long induction times, when the polymerization is carried out in bulk. The offered explanation[4e] was based on the effect of the unreacted $Co(acac)_2$ on the radical dissociation equilibrium (a manifestation of the persistent radical effect). In other words, the radical dissociation equilibrium would lie far on the side of the organocobalt(III) species until nearly all the $Co(acac)_2$ complex is consumed, followed by the established of an equilibrium that is suitably placed to insure a rapid and controlled polymerization process. However, it is hard to accept that a persistent radical effect could result in such a sharp transition for the free radicals concentration. We will herein propose an alternative explanation to account for all the observed data.

The second feature is related to the exact nature of the $Co(acac)_2$ species in solution under the polymerization conditions. The nature of $Co(acac)_2$ in noncoordinating solvents has been addressed by Cotton and Soderberg on the basis of visible and near-IR spectroscopy. The compound is mononuclear tetrahedral in dilute solutions, whereas it affords octahedral coordination through the formation of oligonuclear aggregates at higher concentrations.[11] An early X-ray diffraction study of anhydrous $Co(acac)_2$, obtained by sublimation, showed a tetranuclear $Co_4(acac)_8$ arrangement where octahedral coordination for the Co^{II} ions is achieved by sharing of oxygen donors.[12] A different polymorph, described as containing square-planar mononuclear units, has been characterized more recently.[13] The authors underline the absence of significant intermolecular interactions,

but a closer look at the molecular packing (structure retrieved from the Cambridge Crystallographic Data Centre)[13] reveals that the molecules are in fact loosely stacked on top of each other as shown in ScScheme 2(a). Thus, each Co atom is effectively 6-coordinated, with the 5th and 6th axial coordination positions being occupied by the □-delocalized electron density of the acac ligand of neighboring molecules. A sterically more encumbered analogue, Co[*t*BuC(O)CHC(O)*t*Bu]$_2$, on the other hand, adopts a tetrahedral structure rather than a square planar arrangement, as shown in ScScheme 2(b).[14] It is also known that the addition of small amounts of neutral donors yields complex equilibria. For instance, the addition of pyridine yields complexes having py/Co ratios of 1:2, 1:1 and 2:1, the first two species being described as dinuclear, [Co(acac)$_2$]$_2$(py) and [Co(acac)$_2$(py)]$_2$.[15] Indeed, X-ray crystallography shows that the analogous 1:1 adduct with water is dinuclear, [Co(acac)$_2$(H$_2$O)]$_2$,[16] but a mononuclear 5-coordinate Co(acac)$_2$(ED) adduct (ED = electron donor) has also been crystallographically characterized for ED = 2-aminopyridine.[17] Many EDs have been shown to add to Co(acac)$_2$ and yield 1:2 adducts, Co(acac)$_2$(ED)$_2$. X-ray crystallographic analyses of numerous derivatives (*e.g.* ED = H$_2$O,[16, 18] MeOH,[19] pyridine,[20] imidazole,[21]…), revealed that these complexes have an *trans*-octahedral geometry, as shown in ScScheme 2(c). All these observations indicate the propensity of Co(acac)$_2$ to establish weak coordinative interactions with electron donors leading to octahedral coordination. A reasonable question to ask, therefore, is whether the monomer vinyl acetate might be able to establish a coordinative interaction with Co(acac)$_2$ through the oxygen lone pairs of the ester function, since the bulk CRP of VOAc mediated by Co(acac)$_2$ with V-70 is conducted in the presence of excess VOAc compared to Co(acac)$_2$ ([VOAc]$_0$/[Co]$_0$>100) at 30 ºC.[4e-h]

Insert ScScheme 2

Moreover, the cobalt complex proposed as the dormant species in Scheme 1 (Equation 1, X = $Co(acac)_2$) is only pentacoordinated, whereas Co^{III} is known to strongly prefer a 6-coordinated, octahedral coordination geometry. This suggests that one molecule of reactant or other available ED may occupy the 6^{th} available coordination site. In this report, we explore the molecular structure of the $Co(acac)_2$ complex in solution using ^1H NMR spectroscopy and DFT calculations. The effect of EDs such as py and triethylamine on the $Co(acac)_2$-mediated polymerization of VOAc is also discussed. This work has allowed to correlate the catalytic performance of $Co(acac)_2$ with the nature of EDs and to reveal a previously unsuspected interplay, which is tuned by the ED coordination, between OMRP and DT pathways.

Experimental Section

Characterization. ^1H NMR spectra were collected at 30 ^oC using a Bruker 250 MHz spectrometer. Deuterated benzene and acetone-d_6 were degassed and stocked in a Schlenk tube on molecular sieves, under argon. The vinyl acetate (VOAc) conversion was determined by gas chromatography (GC) using a Shimadzu GC 14-A gas chromatograph equipped with a FID detector and a ValcoBond 30 m VB WAX Megabore column or was calculated by the mass ratio before and after the complete removal of solvent and residual monomer by evaporation, until achievement of constant weight. Toluene or *p*-dimethoxybenzene was used as an internal standard for GC. The molecular weight and

molecular weight distribution of the PVOAc were measured by gel permeation chromatography (GPC) with PSS columns (styrogel 10^5, 10^3, 10^2 Å) and RI detector (molecular weights and polydispersity indices of the PVOAc were determined relative to linear poly(methyl methacrylate) calibration standards using toluene as an internal standard) or with a 300 × 7.5 mm PLgel 5-m Mixed-D column (Polymer Laboratories), equipped with multiangle light scattering (miniDawn Tristar, Wyatt Technology Corp.) and refractive index (RI2000, Soparès) detectors. GPC for the PVOAc was performed using THF as eluent at a flow rate of 1 mL/min at 35 ^{o}C

Materials. Dinitrogen was purified by passing through a column of anhydrous calcium sulfate. Vinyl acetate (Aldrich, >99%) was passed through a neutral alumina column to remove the stabilizer, dried over calcium hydride, distilled under reduced pressure, and degassed with dinitrogen. Pyridine (Fisher Scientific, 99.9%) and triethylamine (NEt_3, Aldrich, 99.5%) were dried over calcium hydride and degassed with dinitrogen or argon. Toluene (Fisher Scientific, >99%) was distilled over sodium/benzophenone and degassed with dinitrogen. Acetone (sds, >99%) was distilled over calcium sulfate and degassed with argon. Heptane (sds, >99,5%) was distilled over calcium hydride and degassed with argon. Bis(acetylacetonate)cobalt(II) ($Co(acac)_2$; Acros, 99%), 2,2'-azobis(4-methoxy-2,4-dimethylvaleronitrile) (V-70; Wako, 96%), *p*-dimethoxybenzene (Aldrich, 99%), and deuterated benzene (Cambridge Isotope Lab, >99.5%D) were used as received.

Initial addition of electron donors to the $Co(acac)_2$-mediated VOAc polymerization with V-70. Generally, the polymerizations were conducted using standard Schlenk techniques. The monomer was deoxygenated by dinitrogen bubbling for 30 min prior to addition to the reaction flask. *p*-Dimethoxybenzene (internal standard for GC, 100 mg), $Co(acac)_2$ (28.0 mg, 1.09×10^{-4} mol) , and V-70 (33.5 mg, 1.09×10^{-4} mol) were placed in a Schlenk flask (25 mL) equipped with a magnetic stirring bar at room temperature. This flask was evacuated in vacuum with cooling in a liquid nitrogen bath and backfilled with dinitrogen. This process was repeated three times with cooling. To this flask, VOAc (5.0 mL, 5.43×10^{-2} mol) and pyridine (0.26 mL, 3.21×10^{-3} mol) were added and the resulting mixture was stirred at room temperature (forming an orange solution). After taking an initial sample for GC, the polymerization was started by heating at 30 ^{o}C. Aliquots were withdrawn periodically by a syringe to follow the kinetics of the polymerization process. After 45 hours, the stirring bar stopped spinning due to the high viscosity of the polymerization medium. The lap samples were diluted with acetone prior to analysis by GC. After the GC measurement, the solvent was changed to THF for GPC. The polymerization in the presence of triethylamine was carried out by an identical procedure, except that NEt_3 (0.45 mL, 3.23×10^{-3} mol) was added instead of pyridine and deoxygenated toluene (0.2 mL) was used as an internal standard for GC.

Addition of electron donors to the ongoing $Co(acac)_2$-mediated VOAc polymerization with V-70. The basic procedure was similar to that described in the preceding section. $Co(acac)_2$ (55.8 mg, 2.17×10^{-4} mol) and V-70 (66.9 mg, 2.17×10^{-4} mol) were placed in a Schlenk flask (25 mL) equipped with a magnetic stirring bar at room

temperature. This flask was evacuated under vacuum with cooling in a liquid nitrogen bath and backfilled with nitrogen. This process was repeated three times with cooling. VOAc (10.0 mL, 1.09×10^{-1} mol) and toluene (0.5 mL) were added to this flask, and the resulting mixture was stirred at room temperature (purple suspension). After taking an initial sample for GC, the mixture was heated at 30 ^{o}C to start the polymerization. Aliquots were withdrawn periodically by a syringe to follow the kinetics of the polymerization process. After 38 h, two 2.5 mL aliquots of the reaction mixture ($Co(acac)_2$, 5.42×10^{-5} mol) were placed into separate deoxygenated Schlenk flasks at room temperature The appropriate amount of electron donor (pyridine (0.13 mL, 1.61×10^{-3} mol) or NEt_3 (0.23 mL, 1.65×10^{-3} mol)) was then injected by syringe. These two flasks and the initial flask were reheated at 30 ^{o}C in the same oil bath in order to continue the polymerization. The lap samples were diluted with acetone prior to analysis by GC. After the GC measurement, the solvent was changed to THF for GPC.

$Co(acac)_2$-mediated VOAc polymerization with PVOAc macroinitiator.

Synthesis of PVOAC End-Capped by Cobalt Complex: $Co(acac)_2$ (26 mg, 1.01×10^{-4} mol) and V-70 (186.8 mg, 6.06×10^{-4} mol) were placed in a Schlenk flask equipped with a magnetic stirring bar at room temperature. This flask was evacuated under vacuum with cooling in a liquid nitrogen bath and backfilled with argon. This process was repeated three times with cooling. VOAc (4.0 mL, 4.34×10^{-2} mol) was added to this flask, and the mixture was heated to 30 ^{o}C to start the polymerization. After 16 h (43% conversion), the polymerization was quenched and VOAc was evaporated under vacuum. The polymer was then dissolved in acetone, (re)precipitated with heptane, filtered and dried under reduced

pressure. The isolated PVOAc obtained as a pink solid (M_n = 8446; PDI = 1.14). The color of the isolated PVOAc was green when wet acetone was used.

Chain extension: The PVOAc end-capped with cobalt, prepared as described above (441 mg, 5.2×10^{-5} mol), was placed in a Schlenk flask equipped with a magnetic stirring bar at room temperature. This flask was evacuated under vacuum with cooling in a liquid nitrogen bath and backfilled with argon. This process was repeated three times with cooling. VOAc (6.0 mL, 6.50×10^{-2} mol) was added to this flask, and the mixture was heated to 30 ^{o}C to start the polymerization. Aliquots were withdrawn periodically by a syringe to follow the kinetics of the polymerization process.

Computational details. All geometry optimizations were performed using the B3LYP three-parameter hybrid density functional method of Becke,[22] as implemented in the Gaussian03 suite of programs.[23] The basis functions consisted of the standard 6-31G** for all light atoms (H, C, O), plus the LANL2DZ function, which included the Hay and Wadt effective core potentials (ECP),[24] for Co. The latter basis set was however augmented with an *f* polarization function (= 0.8) in order to obtain a balanced basis set and to improve the angular flexibility of the metal functions. All geometry optimizations were carried out without any symmetry constraint and all final geometries were characterized as local minima of the potential energy surface (PES) by verifying that all second derivatives of the energy were positive. The unrestricted formulation was used for open-shell molecules. The mean value of the spin of the first-order electron wave function, which is not an exact eigenstate of S^2 for unrestricted calculations on open-shell systems, was considered to identify unambiguously the spin state. The value of $<S^2>$ at convergence

was very close to the expected value of 0.75 for doublets, 2 for triplets, and 3.75 for quartets, indicating minor spin contamination.

Results

^{1}H NMR investigation of Co(acac)$_2$ in the presence of EDs. As discussed in the introduction, Co(acac)$_2$ is known to be capable to add electron donor (ED) molecules, establishing sometimes complex equilibria depending on the nature of the ED and the added amount. We wished to learn more about the interaction of Co(acac)$_2$ and specific ED molecules under polymerization conditions by using spectroscopic tools. Co^{II} coordination compounds are paramagnetic and could in principle be investigated by EPR spectroscopy. However, the rapid spin relaxation associated to the quartet state does not allow the detection of a spectrum at room temperature or above. No EPR studies of Co(acac)$_2$(ED)$_2$ complexes have been reported to the best of our knowledge, and toluene solutions of complex Co(acac)$_2$ itself are described as EPR-silent.[25] We have therefore turned to NMR investigations. Indeed, the rapid relaxation of the electron spin magnetization (conditions leading to very broad EPR resonances) favor the observation of relatively sharp (though paramagnetically shifted) NMR resonances.[26] NMR investigations of Co^{II} acetylacetonate complexes are unprecedented, to the best of our knowledge.

Dissolution of anhydrous Co(acac)$_2$ in C_6D_6 yields a homogeneous purple solution which shows only one very broad resonance centered at ca. -1 ppm ($w_{1/2}$ = 860 Hz), see Figure 1(a). We attribute this resonance to the twelve equivalent CH_3 protons of the acac ligand. The signal corresponding to the CH protons could not be identified. We presume that it is either overshadowed by the broad CH_3 resonance, or broadened beyond detection

and lost in the baseline. Indeed, the metal spin density is probably transmitted more efficiently onto the acac CH proton because it is directly linked to the conjugated Co(acac) system. The addition of VOAc to this solution yields no significant color change and the resulting ^{1}H NMR spectrum is the superposition of the broad $Co(acac)_2$ resonance (with essentially unchanged linewidth and chemical shift) and the sharp resonances of free VOAc. The amount of added VOAc affects only the relative intensity of the free VOAc resonances while it does not significantly affect their chemical shift and linewidth. This observation evidences the absence of a significant $Co(acac)_2$-VOAc interaction.

Insert Figure 1

The addition of py to the $Co(acac)_2$ solution results in an immediate color change from purple to orange, indicating the formation of $Co(acac)_2(py)_x$ adducts. The color of *trans*-$Co(acac)_2(py)_2$ complex was reported to be orange.[20] The color change was accompanied by dramatic changes in the NMR spectrum, see Figure 1(b-d). The free ligand resonance is already visible after the addition of ca. 1 equiv. On the other hand, the $Co(acac)_2$ resonance immediately disappears after the first py addition and is replaced by new resonances for the py adduct(s). This is consistent with the solution equilibria that have previously been established by the spectrophotometric study,[15] as summarized in Scheme 3. According to that study, the first addition leading to $[Co(acac)_2]_2(py)$ is essentially quantitative, whereas the equilibrium constant K_2 is only ca. 2.0. Thus, a significant amount of free py would remain present after the addition of 1 equivalent, together with a mixture of $[Co(acac)_2]_2(py)$, $Co(acac)_2(py)$ and $Co(acac)_2(py)_2$. The resonances of the paramagnetic complexes, as well as that of free py, shift as a function of

the added py amount. This indicates that an exchange occurs between the free and coordinated py molecules, and that this is in the *slow exchange limit*. Note, however, that only one set of resonances is observable for the cobalt complexes. Each resonance of this set becomes sharper and its chemical shift is convergent upon addition of a larger py excess, where the $Co(acac)_2(py)_2$ species is predominant. For each proton, the chemical shift difference ($\Delta\nu$) between different $Co(acac)_2(py)_x$ complexes is likely greater than the $\Delta\nu$ between free and coordinated pyridine. Therefore, the failure to observe individual sets of resonances for the individual cobalt complexes cannot be attributed to fast exchange. It is more likely that the resonances of complexes $[Co(acac)_2]_2(py)$ and $Co(acac)_2(py)$ are not detected because they are broader, less intense (especially at the higher py/Co ratios) and more paramagnetically shifted. The last proposition is proven by the direction in which each resonance shifts as a function of the py/Co ratio. Inspection of the relative integrated intensities, paramagnetic shifts, and line widths leads to the resonance assignment given in Figure 1. It is interesting to note how the acac resonance continuously shifts and sharpens from the value of free $Co(acac)_2$ to that of $Co(acac)_2(py)_2$. This behavior suggests that the observed resonance for pure $Co(acac)_2$ results from the rapid equilibration between mononuclear and oligonuclear species. The small resonance of the *p*-py proton is not visible for the py/Co = 1 spectrum, because it is overshadowed by the stronger acac and free py resonances.

Insert Scheme 3

Contrary to the effect of pyridine and similarly to the effect of VOAc, the addition of NEt_3 to the $Co(acac)_2$ solution results in no significant color change. The NMR behavior,

however, is different from both. After the addition of one equivalent, new broad peaks of relatively small intensity that can be attributed to free NEt_3 become visible, as indicated by the black arrows in Figure 2(a), while a broad resonance is still present in the region of free $Co(acac)_2$ (white arrow). The free NEt_3 resonances, especially the one attributed to the CH_2 group, exhibit a paramagnetic shift (δ 7.86 for CH_2, 0.94 for CH_3; *cf.* 2.50 and 1.06 in the absence of the Co complex). Further addition of a second NEt_3 equivalent affords a very large increase of the free NEt_3 resonances and a shift to δ 7.56 (CH_2) and 0.97 (CH_3), while the broad $Co(acac)_2$ resonance is still present, Figure 2(b). A fourfold amount of NEt_3 produces a further resonance shift to δ 6.66 and 1.01, while the free $Co(acac)_2$ resonance is now essentially disappeared, Figure 2(c). Continued NEt_3 addition further shifts the free Et_3N resonances toward the diamagnetic position (e.g. δ ca. 3.0 for the CH_3 protons after the addition of 30 equivalents). The resonances of the coordinated NEt_3 and acac ligands in complexes $Co(acac)_2(NEt_3)_x$ are not visible. At the same time, the resonance of free $Co(acac)_2$ remains unshifted and unbroadened. These results can be rationalized on the basis of the same scheme invoked for the py system (Scheme 3).[15] The observations prove that NEt_3, like py, forms adducts with $Co(acac)_2$, but the equilibria are far less in favor of the addition products (*i.e.* K_1, K_2 and K_3 are smaller). Like for the py system, an exchange occurs between free and coordinated NEt_3 molecules. A bis adduct forms to a much lower extent or not at all, or its resonances are much broader because of a faster ligand exchange process. The observation of the unshifted $Co(acac)_2$ resonance at low NEt_3/Co ratios shows that this complex is not involved in the amine exchange process. This means that the NEt_3 exchange probably involves the different NEt_3 adducts, rather than dissociation to yield the $Co(acac)_2$ starting compound.

Insert Figure 2

Since water is a possible contaminant of $Co(acac)_2$ and since the VOAc polymerization was also successfully carried out under suspension and miniemulsion conditions,[4f, 4i] additional NMR experiments were carried out by deliberately adding water. The addition of water to a C_6D_6 solution of $Co(acac)_2$ caused the immediate precipitation of a pale solid, presumably $Co(acac)_2(H_2O)_2$, which is described as sparingly soluble in non-polar organic solvents.[16, 18] In order to avoid the precipitation process, subsequent analyses were carried out in acetone-d_6.

First, the spectrum of $Co(acac)_2$ in acetone-d_6 was recorded before the addition of water, see Figure 3(a). This shows two broad ($w_{1/2}$ ca. 400 Hz) resonances at δ ca. 6.8 and 9.4 that can be assigned either to the CH_3 and CH resonances of the acac ligand in a single compound, or to the CH_3 resonances of two different compounds. The latter possibility appears more likely since the CH resonance has not been observed for any of the other spectra (see also below). The nature of the second compound, however, is unclear. The shift and sharpening of the $Co(acac)_2$ resonance from the value observed in C_6D_6 suggests that an interaction with the acetone solvent has taken place. It is interesting to compare this result with the lack of any interaction between $Co(acac)_2$ and VOAc. Evidently, the replacement of the alkoxo group in VOAc by a methyl group in acetone significantly improves the donor properties of the carbonyl function. The subsequent addition of small amounts of water to this solution caused precipitation, indicating that the acetone ligands have been replaced by water molecules. It is also interesting to analyze the spectral changes observed upon addition of NEt_3 in acetone-d_6, see Figure 3(b), and to compare

them with those observed in C_6D_6. The broad resonance centered around δ 6.8 remains visible, even after the addition of 3 equivalents of NEt_3, and does not shift significantly with the amount of excess NEt_3. At the same time, the free NEt_3 resonance is paramagnetically shifted to a lesser extent relative to the corresponding experiment in C_6D_6 (δ 6-7 in acetone-d_6, vs. □ 8-7 in C_6D_6). This is in agreement with the expected smaller extent of NEt_3 coordination to $Co(acac)_2$, since the acetone solvent now competes for the coordination sites on Co^{II}. The broad resonance observed for the $Co(acac)_2$ solution around δ 9.4, on the other hand, is no longer visible. The addition, to this solution, of small amounts of water led again to the formation of a pale precipitate. However, subsequent addition of pyridine caused the redissolution of this precipitate and the formation of an orange solution, whose ^1H NMR spectrum is identical to that shown in Figure 1.

Insert Figure 3

In conclusion, these NMR experiments indicate a relative affinity of various ED molecules for coordination to $Co(acac)_2$ in the order VOAc (no coordination) < NEt_3 < acetone < H_2O < pyridine. They also indicate the presence of an exchange between free and coordinated ED molecules, the rate of exchange being faster for the less strongly coordinated ligands. In the presence of excess ED, the cobalt center undergoes less ligand dissociation and exchange, as evidenced by the relatively sharp paramagnetically shifted resonances in the case of pyridine. For the less tightly bound ligands, the NMR spectrum is not visible and no structural information is furnished by the experiment, but equilibria between lower coordinate species, mono- and/or dinuclear, are probably occurring rapidly.

Computational investigation of the $Co(acac)_2$ structure and interactions with EDs. The adoption of a tetrahedral structure for $Co[tBuC(O)CHC(O)tBu]_2$[14] suggests an electronic preference for a tetrahedral environment around 4-coordinate Co(II), whereas a *trans*-octahedral geometry is adopted in the presence of EDs. However, the steric demand of the *t*Bu substituents may be responsible for this choice. Previous spectrophotometric studies have provided evidence that $Co(acac)_2$ is a tetrahedral monomer, like its *t*Bu analogue, in dilute solution.[11] We have recurred to DFT calculations to further confirm this conclusion. $Co(acac)_2$ was optimized in both the tetrahedral and the square planar geometry. In the former case, only the high spin (S = 3/2) configuration was considered, since no low-spin tetrahedral complex for any d^4-d^7 metal is know with low field ligands.[27] The square planar geometry, on the other hand, generates a high-energy d_{x2-y2} orbital possible resulting in spin pairing, thus both doublet and quartet spin states were considered. The results of the calculations are listed in Table 1. In agreement with the experimental study, the lowest energy is found for the quartet tetrahedral geometry. Although no symmetry was imposed in the calculation, the geometry converged to an essentially perfect D_{2d} symmetry. The optimized Co-O distance (1.945 Å) and O-Co-O angle (95.8°) are quite close to those determined experimentally for $Co[(Bu^tCO)_2CH]_2$ (1.934 Å and 95.4°, respectively).[14b] The square planar geometry gave a stable minimum only in the doublet state, a few kcal mol^{-1} higher than the lower tetrahedral quartet. Attempts to optimize a quartet square planar geometry led to the rearrangement to the tetrahedral minimum.

Insert Table 1

The main thrust of our computational investigation concerns the equilibria affecting the radical concentration under polymerization conditions, and how these are modified by the introduction of electron donors. We have therefore studies the binding of ED molecules to the $Co(acac)_2$ catalyst and to the R-$Co(acac)_2$ dormant species. However, we have limited our investigation to mononuclear complexes. The Co^{III} systems is most likely present in the 6-coordinate R-$Co(acac)_2$(ED) form. Ligand dissociation to give mononuclear R-$Co(acac)_2$ was considered, but the possible dimerization of the latter was not. The activation process generates the mononuclear $Co(acac)_2$(ED) or $Co(acac)_2$ complexes, which may yield dinuclear or oligonuclear aggregates. We have limited our study to the equilibria of the above two mononuclear Co^{II} complexes with each other and with the octahedral complex $Co(acac)_2(ED)_2$. The results of these investigations can at least qualitative address the behavior of the polymerization process under conditions of excess ED. An additional cautionary note concerns the neglect of entropy contributions. A statistical mechanics analysis of the entropic term via the partition function is only possible in the gas phase, whereas the polymerization reactions are carried out in condensed phases. Therefore, the considerations that will be drawn can only be qualitatively based on the bond energy values.

Compound CH_3COOCH_3 was selected as a model for VOAc. Since bonding is established by the carbonyl O atom which is not conjugated with the vinyl function, this replacement is not expected to change the donor properties of the ester function and reduces the computational effort. Pyridine was used as such, whereas NEt_3 was modeled with NMe_3 and NH_3, allowing a partial probing of steric effect. Finally, H_2O was also used as an ED. Concerning the Co^{III} spin trap, CH_3 was chosen as a model for the R group. Although

the resulting R-Co BDE's will be unrealistic, the trends obtained for the different ED molecules should be qualitatively relevant.

The addition of a single ED molecule affords $Co(acac)_2(ED)$ structures with a trigonal bipyramidal geometry, as shown in Table 1. The possibility of the alternative square planar geometry was explored with ED = H_2O, but resulted in a higher energy. All investigated molecules converged to similar trigonal bipyramidal structures in the quartet state. The interaction energy increases in the order $CH_3COOCH_3 < N(CH_3)_3 \sim py < NH_3 < H_2O$. It is interesting to remark the very weak interaction with the carbonyl function of CH_3COOCH_3, whereas NMe_3 and py form Co-N bonds of approximately equal strength. The $Co\text{-}OH_2$ and $Co\text{-}NH_3$ bonds are stronger still. The last two systems exhibit a significant distortion, with one close contact between one of the ED protons and one of the axial acac O atoms (O-H···O = 1.894 Å for ED = H_2O, N-H···O = 2.232 Å for ED = NH_3) suggesting the presence of an H-bonding interaction. In agreement with this hypothesis, the bond angles between the Co-O(N) and O(N)-H bonds are correspondingly smaller than expected (Co-O-H = 91.7° vs. 113.5° for the other O-H bond; Co-N-H = 101.8° vs. 114.0° and 114.2° for the other N-H bonds). This phenomenon may be partially responsible for the additional stability of these adducts relative to the other ED's which lack active protons. However, we must also consider that the stabilization energy is calculated relative to isolated $Co(acac)_2$ and H_2O or NH_3 molecules in the gas phase. In condensed phases (for instance, toluene solution) these protic ED molecules form aggregates, therefore reducing the energetic gain of the $Co\text{-}H_2O$ or $Co\text{-}NH_3$ bond formation. The difference between NH_3 and NMe_3 could in part be due also to the increased steric demand imposed by the three Me groups. By

extrapolation, we can predict that the binding energy of the Co-NEt_3 bond will be smaller relative to the Co-py bond, in agreement with the NMR results.

The above trends remain unchanged upon going to the *trans*-$Co(acac)_2(ED)_2$ systems. As shown in Table 1, binding the second ED molecule results in each case in a slightly greater energy gain relative to the first one, consistent with the general tendency of $Co(acac)_2$ to form octahedral complexes rather than 5-coordinated ones by the addition of ED's. The optimized coordination geometries are in general quite close to octahedral, with the two acac ligands being approximately coplanar. The H_2O and NH_3 adducts exhibit a distortion which consists of a flap of the two acac ligands around the O···O "hinge" axes, in opposite directions. This is particularly evident for the NH_3 derivative, where the hinge angle (angle between the acac plane and the CoO_2 plane) is 158.85°. The reason for this distortion is not obvious, but we note that this is also experimentally observed for the $Co(acac)_2(H_2O)_2$ structure[16] (hinge angle of 162.8° *vs.* 164.0 for the optimized structure). Upon going from the NH_3 to the NMe_3 adduct, the two Co-acac 6-member cycles go back to planarity, suggesting that H-bonding may again be the cause of the distortion. The optimized geometry of the pyridine adduct exhibits the two py orthogonal to each other. This corresponds to the arrangement experimentally observed for *trans*-$Co(acac)_2(py)_2$[20] and for *trans*-$Co(acac)_2(4\text{-}CH_3py)_2$.[28] The optimized Co-O and Co-N distances (averages are 2.06 and 2.23 Å) are in good agreement with the experimentally observed ones (2.034(3) and 2.19(1) Å).[20]

The conclusion of this theoretical investigation is that $Co(acac)_2$ generally forms weak bonds with ED molecules, especially the carbonyl O atom of ester functions. This result is in qualitative agreement with the observation of oxygen-bridged octahedral

coordination for tetrameric $Co(acac)_2$[12] and with the preference of a mononuclear tetrahedral structure for the sterically more encumbered *t*Bu analogue.[14] Amines and pyridine bind more strongly, but the steric bulk of NEt_3 should probably reduce the bond formation energy. The calculations overestimate the stability of the H_2O and NH_3 adducts (indeed, the NMR study proves that H_2O binds less strongly than pyridine), because of the incomplete consideration of hydrogen-bonding interactions (neglected for the free ligands).

Computational investigation of the CH_3-$Co(acac)_2$ bond strength and interactions with EDs.

The salient results of this study are collected in Table 2. The optimization of 5-coordinate CH_3-$Co(acac)_2$ molecule was attempted both as a trigonal bipyramid (*tbp*) and as a square pyramid (*sp*). The *tbp* calculation gave a stable minimum only in the triplet state. Attempts to optimize a *tbp* geometry in the singlet state led to a rearrangement and convergence of the more stable *sp* structure. Relative to the separate tetrahedral (S = 3/2) $Co(acac)_2$ and CH_3 radical, the singlet *sp* was more stable by 18.50 kcal mol^{-1}, whereas the triplet *tbp* was only stabilized by 6.52 kcal mol^{-1}. The Co^{III} ion is known to be particularly stable in an octahedral coordination environment, thus the presence of ED molecules is expected to lead to dormant species of type $Co(acac)_2$(PVOAc)(ED). The various ED molecules were added to the empty coordination site of the lower-energy *sp* CH_3-$Co(acac)_2$ molecule to yield *trans*-$Co(acac)_2(CH_3)$(ED) adducts. All these molecules were optimized only in the singlet state, as alkylcobalt(III) molecules are known to be diamagnetic.[29] Note, however, that no R-$Co(acac)_2$ or R-$Co(acac)_2$(ED) molecules have been previously described to the best of our knowledge. Axial ED binding to either CH_3-$Co^{III}(acac)_2$ or to

$Co^{II}(acac)_2(ED)$ results in very similar energetic gains for CH_3COOCH_3 (4.23 vs. 4.49 kcal mol^{-1}), H_2O (11.53 vs. 11.47 kcal mol^{-1}) and NH_3 (13.47 vs. 13.67 kcal mol^{-1}). On the other hand, slightly stronger binding to the alkylcobalt(III) occurs for NMe_3 (7.41 vs. 5.63 kcal mol^{-1}) and especially for py (9.10 vs. 5.63 kcal mol^{-1}).

Insert Table 2

The stereoelectronic properties of ED could affect the homolytic bond strength of the Co^{III}-carbon bond (that is, on the energy difference between $Co(acac)_2(CH_3)(ED)$ and the separate $Co(acac)_2(ED)$ and CH_3 fragments), as previously demonstrated in the chemistry of vitamin B_{12}.[30] However, the axial ED nature has only a slight effect on the Co^{III}-CH_3 BDE for this system: 21.82 kcal mol^{-1} for CH_3COOCH_3, 20.65 kcal mol^{-1} for NMe_3, 21.83 kcal mol^{-1} for py, 22.65 kcal mol^{-1} for H_2O and 21.80 for NH_3. All these values are greater than the Co^{III}-CH_3 BDE of unsolvated $Co(acac)_2(CH_3)$ (18.50 kcal mol^{-1}).

It is interesting to compare two processes of relevance to the radical polymerization controlled by $Co(acac)_2$: on the one side, the homolytic CH_3-Co bond rupture in the octahedral complex CH_3-$Co(acac)_2(ED)$; on the other side, the equilibrium between the resulting 5-coordinate $Co(acac)_2(ED)$ complex and the corresponding bis-adduct, $Co(acac)_2(ED)_2$. For each ED used in the computational study, the energetics of these two processes are shown on the left and right hand sides of Figure 4, respectively. The absolute values are not useful for evaluating the equilibrium positions and the effective polymerization rates for a variety of reasons (CH_3 model for the growing polymer chain, neglect of entropy, …). The free energies are in principle less positive for the homolytic bond rupture process and less negative for the ED addition process, relative to the energies

shown in Figure 4. However, the figure allows the estimation of qualitative trends. Under the hypothesis of identical entropic contributions for the different ED systems, a greater Co-CH_3 BDE should slow down the effective polymerization rate, whereas a greater stabilization by the ED addition should accelerate the process. The latter phenomenon results from the reduced availability of the $Co(acac)_2$(ED) radical trap and from the fact that the coordinatively saturated $Co(acac)_2(ED)_2$ complex has no trapping ability. Therefore, the kinetic acceleration may also be accompanied by partial or total loss of control.

Insert Figure 4

Effect of the initial addition of electron donors on the CMRP of VOAc mediated by $Co(acac)_2$ with V-70. As demonstrated above, N-donor ligands such as py and NEt_3 are able to coordinate to a different extent to $Co(acac)_2$ (py >> NEt_3), producing $Co(acac)_2(ED)_x$ complex. There is no indication, on the other hand, for the coordination of VOAc to $Co(acac)_2$. Therefore, an electron-donating effect originating from the coordinating ED may change the reactivity of cobalt(II) complex towards a VOAc radical. Accordingly, 30 equiv of EDs (py or NEt_3) compared to cobalt were initially added to the $Co(acac)_2$-mediated VOAc polymerization initiated by V-70 at 30 ^oC ($[VOAc]_0/[Co(acac)_2]_0/[V\text{-}70]_0/[ED]_0$ = 500/1/1/30). In the absence of ED additives, the initial color of the reaction medium was a purple slurry, and then it changed to a brown solution after 1 day, suggesting the formation of cobalt(III) species. A rapid polymerization started after an induction period (see the semilogarithmic plot in Figure 5) and the number average molecular weight increased more or less linearly with conversion, with relatively low polydisperties (see Figure 6). The raw data are also reported in tabular form as

Supporting Information. The observed M_n are close to (slightly higher than) those expected for one growing chain per cobalt atom. All these observations are in line with the previous report.[4e] Note that our reaction conditions are identical with those used previously, except that we employed a V-70/Co ratio of 1:1 instead of 6.5:1. Consequently, the only major difference of our results with respect to those previously reported is the longer observed induction time (ca. 30 h).

Insert Figure 5 and Figure 6

For the experiment run in the presence of py (30 equiv), the purple slurry turned immediately to a clear orange solution, as described above. The mixture remained a clear orange solution until the end of polymerization. While this may suggest the persistence of the Co(II) species during the polymerization, note that R-Co(acac)$_2$(ED) compounds have not previously been described, thus the formation of alkylcobalt(III) dormant species that would coincidentally have the same color cannot be excluded. In the case of NEt_3, the reaction medium quickly turned to a violet colored slurry, and then it became a mixture of a brown solution and pale purple insoluble materials after 1 day. The semilogarithmic kinetic plots for the monomer consumption are shown in Figure 5. The first striking observation is that, in the presence of py or NEt_3, the polymerizations did not show any induction period. The linearity of the plots suggests that the polymerizations are controlled, which is further confirmed by the evolution of M_n and M_w/M_n versus monomer conversion (see Figure 6). For both polymerizations, M_n increased with conversion and remained close to the theoretical values, while the polydispersity remained in the 1.3 – 1.5 range and all of the

GPC curves displayed a monomodal shape (representative chromatograms are available as Supporting Information). Although these values are higher than for the PVOAc prepared in the absence of ED, they are typical of CRP processes. The significance of the M_n growth for ED = NEt_3 is limited, since the polymerization was very slow and only low conversions (up to 14%) were achieved. However, the isolated polymers had M_n in close agreement with the theoretical values, under the assumption that only one macromolecular chain is generated per cobalt atom. In the case of py, the M_n of PVOAc exhibited a larger departure from the $M_{n,th}$ toward greater values, showing that less than one chain per cobalt is generated. The phenomenon is likely resulting from a combination of slow initiation (the half-life of V-70 is ca. 10 h at 30°C) and inefficient trapping of the radicals generated by V-70 by the Co^{II}-py system.

Effect of the addition of electron donors to an ongoing CMRP of VOAc mediated by $Co(acac)_2$ with V-70. In order to further explore the effect of ED coordination to the dormant species on the $Co(acac)_2$-mediated VOAc polymerization, excess ED was added to the reaction system after the formation of the dormant species. First, a normal CRP of VOAc was conducted at 30°C to prepare a dormant species having a PVOAc chain ($[VOAc]_0/[Co(acac)_2]_0/[V\text{-}70]_0$=500/1/1). After 43 h, the reaction medium (brown solution) was split into three equal parts, and 30 equiv of py or NEt_3 compared to $Co(acac)_2$ were injected into two of these mixtures. Subsequently, all three mixtures were reheated at 30 °C in the same bath to continue the polymerization. Figure 7 shows the semilogarithmic kinetic plot, whereas Figure 8 reports the evolution of M_n and M_w/M_n versus conversion. The data are available in tabular form as Supporting Information.

Because the half-life of V-70 in toluene at 30°C is 10 h, almost of all V-70 should have already decomposed after 43 h. Therefore, the predominant compound in the polymerization system will be the $Co(acac)_2$(PVOAc) complex as a dormant species, with the possible additional coordination of a VOAc monomer molecule. After the addition of 30 equiv of py, the color of reaction medium immediately changed from a brown solution to a clear orange solution, as was the case for initial addition of py to the reaction medium. Moreover, this mixture became more viscous within 1 h, suggesting the production of polymeric materials. In contrast, no color change was observed in the case of the NEt_3 addition. As shown in Figure 7, the semilogarithmic kinetic plot after the addition of excess py displayed the faster rate of polymerization relative to the normal CRP of VOAc. This suggested that the formation of $Co(acac)_2$(PVOAc)(py) complex led to the release of PVOAc radicals from the dormant species, resulting in an acceleration of the polymerization rate. On the other hand, the rate of polymerization in the presence of excess NEt_3 was slower than that of the normal CRP, despite no color change. This implies that the coordination of NEt_3 to the dormant species suppressed the dissociation of the cobalt-PVOAc bond. The evolution of M_n and M_w/M_n versus conversion (Figure 8) is much the same as when the ED molecule was introduced at the beginning, before the formation of the dormant species (Figure 6), and the molecular weight distribution is once again monomodal (representative chromatograms are available as Supporting Information). These experiments indicate that the addition of the ED molecule changes dramatically the nature of the dormant species but its effect does not depend upon whether the organocobalt(III) compound is generated in its absence or in its presence.

Insert Figure 7 and Figure 8

Interplay of OMRP and DT mechanisms. The controlled growth of PVOAc for the $Co(acac)_2$-mediated polymerization in the presence of py or NEt_3, even though the control is not as good as for the polymerization in the absence of ED, strongly suggests that the cobalt complex interacts with the growing chain, establishing an equilibrium with a dormant species. The dramatic difference in polymerization rate as a function of ED (py >> NEt_3) confirms that the cobalt complex is directly implicated in this equilibrium. On the basis of the solution NMR investigation and the DFT calculations, it is natural to propose that this control is established via an OMRP equilibrium, namely involving the formation of an organometallic dormant species, as shown in Scheme 4 (part b). The reason for the relative polymerization rate in the order py >> NEt_3 can be attributed to the different stabilization of the product of Co^{III}-R bond cleavage, the 5-coordinate Co^{II} complex $Co(acac)_2$(ED), upon coordination of a second ED molecule. The NMR investigation indicates that the py addition is more favorable than the NEt_3 addition and the DFT calculations confirm this trend, after consideration of the steric factors from the result of the NMe_3 model system (Figure 4). In addition, the DFT calculations show that the homolytic bond dissociation energy of the Co^{III}-R bond does not greatly change as a function of the ED.

It should be mentioned that, according to the literature,[31] NEt_3 slows down the free radical polymerization of VOAc because of sacrificial H atom transfer from NEt_3 to the growing radical chain. Since the resulting Et_2NCHCH_3 radical is highly stabilized and is not capable to reinitiate polymerization, this process effectively amounts to a termination

event. However, a control experiment carried out under the same conditions used for the $Co(acac)_2$ mediated polymerization (bulk, $[VOAc]_0/[V\text{-}70]_0/[NEt_3]_0$ = 500/1/30, 30°C) showed that the polymerization rate was only halved, relative to the free polymerization in the absence of NEt_3. Therefore, the sacrificial H atom transfer from NEt_3 may only account for a small fraction of the dramatic polymerization rate decrease on going from py to NEt_3.

The NMR and DFT studies also indicate that vinyl acetate does not establish a significant interaction with $Co(acac)_2$. These results allow us to predict that the spin trap in the absence of ED additive is the simple mononuclear tetrahedral $Co(acac)_2$ complex (perhaps in equilibrium with a higher aggregate, according to the literature[11]). Consequently, the spin trap should not enjoy any particular energetic stabilization in the absence of ED, the equilibrium should be more displaced toward the organocobalt(III) dormant species, and the polymerization should be slower. This indeed corresponds to the experimental evidence at the initial stages of the polymerization process (during the induction period in the absence of ED), but does not account for the fast and controlled polymerization after the initial period.

A reasonable explanation for the latter phenomenon must therefore be based on a different mechanism. The radical influx from the V-70 initiator ($t_{1/2}$ = 10 h at 30°) will gradually convert the $Co(acac)_2$ complex to an organocobalt(III) species in an essentially irreversible process. Toward the end of the transformation of the Co^{II} to the Co^{III} species, the new radicals will no longer be efficiently trapped and will therefore start to generate polymer chains, explaining the onset of a fast polymerization process. The fact that the polymerization remains controlled can be explained by the intervention of a degenerative transfer (DT) process, as indicated in Scheme 4 (part a). The same control mechanism has

been proposed recently for the polymerization of methyl acrylate, acrylic acid, and vinyl acetate by a cobalt porphyrin system.[10] Note that no degenerative transfer mechanism may take place in the presence of ED, because ED blocks the coordination site on the organocobalt(III) dormant species that is necessary for the associative radical exchange. The ED dissociation process from the dormant species (indicated with dashed arrows in Scheme 4) is expected to be slow, because of the well known inertness of low-spin d^6 coordination compounds. Thus, a DT mechanism may only take place when the ED does not strongly bond the Co^{III} dormant species, leaving a significant amount of 5-coordinate $R_0(VOAc)_n$-$Co^{III}(acac)_2$ at equilibrium. Conversely, d^7 complexes are kinetically labile, thus the ED addition/dissociation equilibrium between $Co(acac)_2(ED)$ and $Co(acac)_2(ED)_2$ is kinetically competent to stabilize the Co^{II} spin trap and thereby accelerate the polymerization by the OMRP mechanism.

Insert Scheme 4

In order to find supporting evidence for the presence of a DT process, we have carried out additional polymerizations with different V-70/Co ratios. If the control mechanism were of OMRP type, the apparent rate of polymerization, k_{app}, should follow Equation 1 and thus be independent on the radical influx from the initiator. For a DT mechanism, on the other hand, the polymerization rate should follow an expression like Equation 2 as in free radical polymerization, the rate of exchange k_{exch} affecting only the degree of control.[2] The results of the VOAc polymerization in the presence of different amounts of V-70 are shown in Figure 9. As expected, the induction time decreases for a greater V-70 concentration,

because the greater radical influx allows a faster conversion of the $Co(acac)_2$ into the organocobalt(III) species. Figure 9 shows that the polymerization rate increases when the radical influx increases. The observed pseudo-1st order rate constants are $2.24 \cdot 10^{-3}$ s^{-1} for [V-70]/[Co^{II}] = 4 and $1.04 \cdot 10^{-3}$ s^{-1} for [V-70]/[Co^{II}] = 2. Given an estimated initiator efficiency factor of 0.6 for V-70 and the irreversible consumption of 1 equiv of radicals to convert all Co^{II} to Co^{III}, the residual radical/metal ratios are 3.8 and 1.4, respectively. The ratio of the observed rate constants, $2.24 \cdot 10^{-3}/1.04 \cdot 10^{-3} = 2.15$, is close to the square root of the radical concentration ratio, $(3.8/1.4)^{0.5} = 1.65$. This is as expected for a DT mechanism and disagrees with an OMRP mechanism.

$$k_{app} = (k_p[VOAc])(k_{act}/k_{deact})[R_0(VOAc)_n\text{-}Co^{III}(acac)_2(ED)]/[Co^{II}(acac)_2(ED)]$$

Equation 1

$$k_{app} = (k_p[VOAc])(fk_d[V\text{-}70]/k_t)^{1/2}$$

Equation 2

Insert Figure 9

One strong point that was previously put forward in favor of an OMRP mechanism is the fact that the isolated and purified polymer (described as a green material),[4e, 4h] supposedly end-capped with the $\text{-}Co^{III}(acac)_2$ fragment, can undergo chain extension upon treatment with fresh VOAc and in the absence of new radical source.[4e] This result can only be achieved for an OMRP mechanism, since the DT mechanism relies on the

continuous influx of radicals from an external initiator. We have noted that the reaction mixture maintains a pale brown-pink color during the polymerization procedure and that the polymer, when isolated and purified under rigorous air-free and dry conditions, is pink. However, the aliquots withdrawn from the reaction mixtures for the purpose of calculating the conversion and analyzing the polymer by SEC, turned green during the drying procedure in air. In addition, when the polymer was purified by dissolution in dry acetone and reprecipitation with dry heptane, it maintained its pink color, whereas when the procedure was carried out in the same manner but without using special precautions (regular acetone and in air), the polymer became green. We advance the hypothesis that the pink organocobalt(III) dormant species, generated in the absence of ED, contains 5-coordinate chain ends, $R_0(VOAc)_n$-$Co(acac)_2$ and that the contact with moist air changes the chemical structure of the chain end, changing the color of the material to green. The color change may result from water binding to yield a 6-coordinate chain-end, $R_0(VOAc)_n$-$Co(acac)_2(H_2O)$, or from an oxidation process. The second possibility appears more likely, since no color change occurred when degassed water was added under an inert atmosphere. The chemical nature of this green chromophore is currently unknown and will be investigated at a later time. Since we have demonstrated that ED coordination renders the homolytic dissociation of the organocobalt(III) dormant species easier, and since the DFT calculations indicate that water is able to provide sufficient stabilization of the Co^{II} spin trap, a polymer terminated by -$Co(acac)_2(H_2O)$ chain-ends would be able to undergo chain extension by the OMRP mechanism. In order to test this hypothesis, we have isolated, under as rigorous conditions as possible, a pink poly(vinyl acetate) obtained by the V-70-initiated, $Co(acac)_2$-mediated polymerization in the absence of ED additives (M_n = 18800).

Subsequently, this polymer was treated with additional fresh VOAc in bulk at 35°C and without V-70. No significant polymerization took place over one day (ca. 2% after 1566 min, see Figure 10) while the color of the mixture remained pale pink. At this point, water was deliberately added to the reaction mixture and a faster polymerization process ensued (17% in the subsequent 1300 min). This result demonstrates that the pink $Co^{III}(acac)_2$-capped dormant chain is not capable to chain extend in the absence of a fresh radical source but does so after the addition of water. Therefore, it suggests that the previously reported[4e] chain extension experiment indeed occurs via OMRP as the authors suggested, but this involves a chemically modified organocobalt(III) chain end, after exposure to moist air.

A final point of discussion is the possibility that the associative radical exchange involves an intermediate dialkylcobalt(IV) complex, lying in a more or less deep local energy minimum (see Figure 11). If the associative species in only a transition state, characterized by one normal mode of vibration with an imaginary frequency (case *a* of Figure 11), the mechanism is that of a typical degenerative transfer and the control of polydispersity is only ensured by kinetic factors.[2] If, on the other hand, a stable intermediate dialkyl Co(IV) species exists (case *c* of Figure 11), then we fall back into an OMRP mechanism, the Co(IV) complex being the depository of the dormant polymer chain. In an intermediate situation (case *b* of Figure 11) the Co(IV) intermediate is unstable but has a certain lifetime and will help to insure a better chain grown control. It should be mentioned that at least one sufficiently stable alkylcobalt(IV) complex for isolation and characterization, $Co(norbornyl)_4$, is known, though its stability may be attributed to the severe steric encumbrance of the ligand coordination sphere.[32] For the present system, an aliquot of the reaction mixture did not reveal any EPR signal after quenching to the liquid

N_2 temperature. Thus, it seems that the dialkyl Co^{IV} species is either a transition state or an intermediate with a too short lifetime for measurement by this technique.

Conclusion

The present study has shown that the $Co(acac)_2$-mediated polymerization of VOAc may occur by either one of two fundamentally different mechanism: a degenerative transfer in the absence of ligands capable to establish strong interactions with the cobalt center, i.e. when the $R_0(VOAc)_n$-$Co^{III}(acac)_2$ dormant species remains 5-coordinated, and a reversible homolytic cleavage of the dormant organocobalt(III) species in the presence of strongly binding electron donors, i.e. when the dormant species is 6-coordinated, $R_0(VOAc)_n$-$Co^{III}(acac)_2(ED)$. The second mechanism is accelerated by more strongly binding ED, because of the energetic stabilization of the Co^{II} spin trap due to the formation of 6-coordinated $Co(acac)_2(ED)_2$. On the other hand, no degenerative transfer is possible in the presence of ED, because the latter blocks the coordination site that is necessary for the associative radical exchange. Future efforts in our laboratories will be directed at the synthesis, isolation and characterization of simple model complexes of the organocobalt(III) dormant chain, and to applying the ED modulation of the $Co(acac)_2$ reactivity to the development of new polymeric architectures.

Acknowledgments

KM greatly appreciates the financial support from the National Science Foundation (DMR-0549353 and CHE-0405627), Mitsui Chemicals, Inc. and CRP Consortium at

Carnegie Mellon University. RP thanks the ANR (Contract No. NT05-2_42140) and CINES and CICT (Project CALMIP) for granting free computational time.

References

[1] aK. Matyjaszewski, *Controlled/Living Radical Polymerization: From Synthesis to Materials.*, ACS Symposium Series Vol. 944, American Chemical Society, Washington, DC, **2006**; bK. Matyjaszewski, T. P. Davis, *Handbook of Radical Polymerization*, Wiley-Interscience, Hoboken, NJ, **2002**.

[2] A. Goto, T. Fukuda, *Progress in Polymer Science* **2004**, *29*, 329-385.

[3] C. J. Hawker, A. W. Bosman, E. Harth, *Chemical Reviews (Washington, D. C.)* **2001**, *101*, 3661-3688.

[4] aB. B. Wayland, G. Poszmik, S. L. Mukerjee, M. Fryd, *J. Am. Chem. Soc.* **1994**, *116*, 7943-7944; bB. B. Wayland, L. Basickes, S. Mukerjee, M. Wei, M. Fryd, *Macromolecules* **1997**, *30*, 8109-8112; cL. D. Arvanitopoulos, M. P. Greuel, B. M. King, A. K. Shim, H. J. Harwood, in *Controlled Radical Polymerization, Vol. 685* (Ed.: K. Matyjaszewski), ACS Symposium Series, American Chemical Society, Washington, DC, **1998**, p. 316; dZ. Lu, M. Fryd, B. B. Wayland, *Macromolecules* **2004**, *37*, 2686-2687; eA. Debuigne, J.-R. Caille, R. Jerome, *Angewandte Chemie, International Edition* **2005**, *44*, 1101-1104; fA. Debuigne, J.-R. Caille, C. Detrembleur, R. Jerome, *Angewandte Chemie, international edition* **2005**, *44*, 3439-3442; gA. Debuigne, J.-R. Caille, N. Willet, R. Jerome, *Macromolecules* **2005**, *38*, 9488-9496; hA. Debuigne, J.-R. Caille, R. Jerome, *Macromolecules* **2005**, *38*, 5452-5458; iC. Detrembleur, A. Debuigne, R. Bryaskova, B. Charleux, R. Jerome, *Macromol. Rapid Comm.* **2006**, *27*, 37-41; jR. Poli, *Angew. Chem. Int. Ed. Engl.* **2006**, *45*, 5058–5070.

[5] aJ.-S. Wang, K. Matyjaszewski, *J. Am. Chem. Soc.* **1995**, *117*, 5614-5615; bJ.-S. Wang, K. Matyjaszewski, *Macromolecules* **1995**, *28*, 7901-7910; cT. E. Patten, J. Xia, T. Abernathy, K. Matyjaszewski, *Science* **1996**, *272*, 866-868; dM. Kamigaito, T. Ando, M. Sawamoto, *Chem. Rev.* **2001**, *101*, 3689-3745; eK. Matyjaszewski, J. Xia, *Chem. Rev.* **2001**, *101*, 2921-2990.

[6] aS. G. Gaynor, J.-S. Wang, K. Matyjaszewski, *Macromolecules* **1995**, *28*, 8051-8056; bM. C. Iovu, K. Matyjaszewski, *Macromolecules* **2003**, *36*, 9346-9354.

[7] S. Yamago, *Journal of Polymer Science, Part A: Polymer Chemistry* **2006**, *44*, 1-12.
[8] J. Chiefari, E. Rizzardo, in *Handbook of Radical Polymerization* (Eds.: K. Matyjaszewski, T. P. Davis), Wiley-Interscience, Hoboken, NJ, **2002**, pp. 629-690.
[9] P. Corpart, D. Charmot, T. Biadatti, S. Z. Zard, D. Michelet, in *PCT Int. Appl.; WO9858974*, Rhodia, France, **1998**.
[10] aB. B. Wayland, X.-F. Fu, Z. Lu, M. Fryd, *Polym. Prepr.* **2005**, *230th ACS National Meeting, August 28-September 1, 2005, Washington, DC*; bB. B. Wayland, X. Fu, C.-H. Peng, Z. Lu, M. Fryd, *ACS Symp. Ser* **2006**, *944*, 358-371.
[11] F. A. Cotton, R. H. Soderberg, *Inorg. Chem.* **1964**, *3*, 1-5.
[12] F. A. Cotton, R. C. Elder, *Inorg. Chem.* **1965**, *4*, 1145-1151.
[13] J. Burgess, J. Fawcett, D. R. Russell, S. R. Gilani, *Acta Crystallographica, Section C: Crystal Structure Communications* **2000**, *C56*, 649-650.
[14] aF. A. Cotton, J. S. Wood, *Inorg. Chem.* **1964**, *3*, 245-251; bL.-C. Wang, H.-Y. Jang, Y. Roh, V. Lynch, A. J. Schultz, X. Wang, M. J. Krische, *J. Am. Chem. Soc.* **2002**, *124*, 9448-9453.
[15] J. P. Fackler, Jr., *Inorg. Chem.* **1963**, *2*, 266-270.
[16] F. A. Cotton, R. C. Elder, *Inorg. Chem.* **1966**, *5*, 423-429.
[17] M. Doering, H. Goerls, E. Uhlig, *Zeitschrift fuer Anorganische und Allgemeine Chemie* **1991**, *603*, 7-14.
[18] G. J. Bullen, *Acta Cryst.* **1959**, *12*, 703-708.
[19] P. Werndrup, V. G. Kessler, *Journal of the Chemical Society, Dalton Transactions* **2001**, 574-579.
[20] R. C. Elder, *Inorganic Chemistry* **1968**, *7*, 1117-1123.
[21] M. Doering, W. Ludwig, E. Uhlig, S. Wocadlo, U. Mueller, *Zeitschrift fuer Anorganische und Allgemeine Chemie* **1992**, *611*, 61-67.
[22] A. D. Becke, *J. Chem. Phys.* **1993**, *98*, 5648-5652.
[23] M. J. Frisch, G. W. Trucks, H. B. Schlegel, G. E. Scuseria, M. A. Robb, J. R. Cheeseman, J. Montgomery, J. A., T. Vreven, K. N. Kudin, J. C. Burant, J. M. Millam, S. S. Iyengar, J. Tomasi, V. Barone, B. Mennucci, M. Cossi, G. Scalmani, N. Rega, G. A. Petersson, H. Nakatsuji, M.

Hada, M. Ehara, K. Toyota, R. Fukuda, J. Hasegawa, M. Ishida, T. Nakajima, Y. Honda, O. Kitao, H. Nakai, M. Klene, X. Li, J. E. Knox, H. P. Hratchian, J. B. Cross, C. Adamo, J. Jaramillo, R. Gomperts, R. E. Stratmann, O. Yazyev, A. J. Austin, R. Cammi, C. Pomelli, J. W. Ochterski, P. Y. Ayala, K. Morokuma, G. A. Voth, P. Salvador, J. J. Dannenberg, V. G. Zakrzewski, S. Dapprich, A. D. Daniels, M. C. Strain, O. Farkas, D. K. Malick, A. D. Rabuck, K. Raghavachari, J. B. Foresman, J. V. Ortiz, Q. Cui, A. G. Baboul, S. Clifford, J. Cioslowski, B. B. Stefanov, G. Liu, A. Liashenko, P. Piskorz, I. Komaromi, R. L. Martin, D. J. Fox, T. Keith, M. A. Al-Laham, C. Y. Peng, A. Nanayakkara, M. Challacombe, P. M. W. Gill, B. Johnson, W. Chen, M. W. Wong, C. Gonzalez, J. A. Pople, *Gaussian 03, Revision B.04*, Gaussian, Inc., Wallingford CT, **2003**.

[24] P. J. Hay, W. R. Wadt, *J. Chem. Phys.* **1985**, *82*, 270-283.

[25] F. K. Shmidt, L. O. Nindakova, B. A. Shainyan, V. V. Saraev, N. N. Chipanina, V. A. Umanetz, *J. Mol. Catal. A* **2005**, *235*, 161-172.

[26] aG. N. La Mar, W. D. Horrocks, Jr., R. H. Holm, *NMR of paramagnetic molecules*, Academic Press, New York, **1973**; bI. Bertini, C. Luchinat, *Coord. Chem. Rev.* **1996**, *150*, 1-296.

[27] J. E. Huheey, E. A. Keiter, R. L. Keiter, *Inorganic Chemistry. Principles of Structure and Reactivity*, 4th ed., Harper & Row, New York, **1993**.

[28] A. P. Gulya, G. V. Novitskii, S. G. Shova, M. D. Mazus, I. Sandu, *Koordinatsionnaya Khimiya* **1993**, *19*, 227-231.

[29] D. Dodd, M. D. Johnson, *Journal of Organometallic Chemistry* **1973**, *52*, 1-232.

[30] aJ. Halpern, *Science* **1985**, *227*, 869-876; bK. P. Jensen, U. Ryde, *J. Am. Chem. Soc.* **2005**, *127*, 9117-9128.

[31] N. M. Beileryan, R. G. Melkonyan, O. A. Chaltykyan, *Armyanskii Khimicheskii Zhurnal* **1971**, *24*, 203-206.

[32] aB. K. Bower, H. G. Tennent, *J. Am. Chem. Soc.* **1972**, *94*, 2512-2514; bB. K. Bower, M. Findlay, C. W. Chien, *Inorg. Chem.* **1974**, *1974*, 759-761.

[33] L.-C. Wang, H.-Y. Jang, Y. Roh, V. Lynch, A. J. Schultz, X. Wang, M. J.

Krische, *J. Am. Chem. Soc.* **2002**, *124*, 9448-9453.

Figure captions

Figure 1. ^{1}H NMR spectra of (a) VOAc, (b) the mixture of $Co(acac)_2$ with 10 equiv of VOAc, and (c) the mixture of $Co(acac)_2$ with 100 equiv of VOAc, in C_6D_6 at 30 ^oC (300 MHz).

Figure 2. ^{1}H NMR spectra of (a) the mixture of $Co(acac)_2$ with 10 equiv of VOAc, (b) (a)+Py (10 equiv), and (c) (a)+Py (30 equiv), in C_6D_6 at 30 ^oC (300 MHz).

Figure 3. ^{1}H NMR spectra of (a) the mixture of $Co(acac)_2$ with 10 equiv of VOAc, (b) (a)+NEt_3 (10 equiv), and (c) (a)+ NEt_3 (30 equiv), in C_6D_6 at 30 ^oC (300 MHz).

Figure 4. Semilogarithmic kinetic plots for the initial addition of electron donors to bulk CMRP of VOAc mediated by $Co(acac)_2$ with V-70 at 30 ^oC.: (■) No addition, (●) Addition of py (30 equiv), (▲) Addition of NEt_3 (30 equiv), $[VOAc]_0/[Co(acac)_2]_0/[V\text{-}70]_0/[ED]_0=500/1/1/30$.

Figure 5. Evolution of M_n and M_w/M_n versus conversion for the initial addition of electron donors to bulk CMRP of VOAc mediated by $Co(acac)_2$ with V-70 at 30 ^oC.: (■, □) No addition, (●, ○) Addition of py (30 equiv), (▲, Δ) Addition of NEt_3 (30 equiv), $[VOAc]_0/[Co(acac)_2]_0/[V\text{-}70]_0/[ED]_0=500/1/1/30$.

Figure 6. GPC traces of PVOAc prepared by the initial addition of electron donors to bulk CMRP of VOAc mediated by $Co(acac)_2$ with V-70 at 30 ^oC.: (a) Addition of py (30 equiv), (b) Addition of NEt_3 (30 equiv), $[VOAc]_0/[Co(acac)_2]_0/[V\text{-}70]_0/[ED]_0=500/1/1/30$.

Figure 7. Semilogarithmic kinetic plots for the middle addition of electron donors to bulk CMRP of VOAc mediated by $Co(acac)_2$ with V-70 at 30 ^oC.: (■) No addition, (●) Addition of py (30 equiv), (▲) Addition of NEt_3 (30 equiv), $[VOAc]_0/[Co(acac)_2]_0/[V\text{-}70]_0/[ED]_0=500/1/1/30$.

Figure 8. Evolution of M_n and M_w/M_n versus conversion for the later addition of electron donors to bulk CMRP of VOAc mediated by $Co(acac)_2$ with V-70 at 30 ^oC.: (■, □) No

addition, (●, ○) Addition of py (30 equiv), (▲, Δ) Addition of NEt_3 (30 equiv), $[VOAc]_0/[Co(acac)_2]_0/[V\text{-}70]_0/[ED]_0=500/1/1/30$.

Figure 9. GPC traces of PVOAc prepared by the middle addition of electron donors to bulk CMRP of VOAc mediated by $Co(acac)_2$ with V-70 at 30 ºC.: (a) Addition of py (30 equiv), (b) Addition of NEt_3 (30 equiv), $[VOAc]_0/[Co(acac)_2]_0/[V\text{-}70]_0/[ED]_0=500/1/1/30$.

Scheme caption.

Scheme 1. General Mechanisms for Three Controlled/"Living" Radical Polymerizations.

Scheme 2. Proposed Polymerization Mechanism for Radical Polymerization Mediated by $Co(acac)_2$ Complex.

Scheme 3. Proposed General Mechanism for the CMRP of VOAc Mediated by $Co(acac)_2$ Complex in the Presence of Excess Electron Donors.

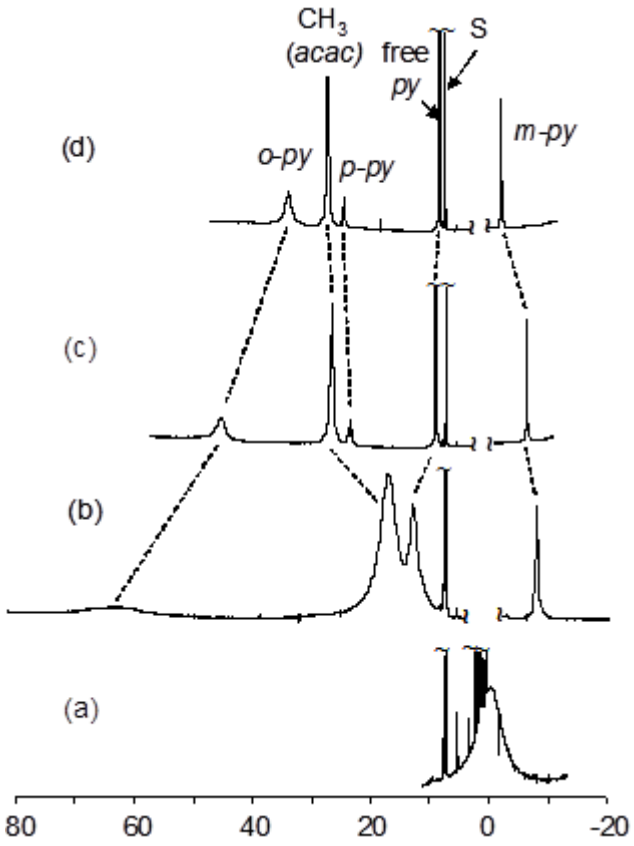

Figure 1. ^{1}H NMR spectra in C_6D_6 of the mixture of $Co(acac)_2$ with py: (a) no added ligand; (b) 1 equiv; (c) 2 equiv; (d) 3 equiv.

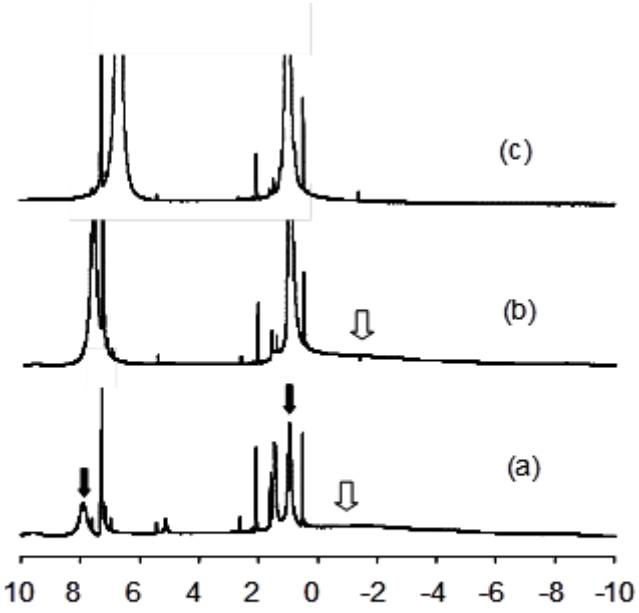

Figure 2. ^{1}H NMR spectra in C_6D_6 of the mixture of $Co(acac)_2$ with NEt_3: (a) 1 equiv; (b) 2 equiv; (c) 4 equiv.

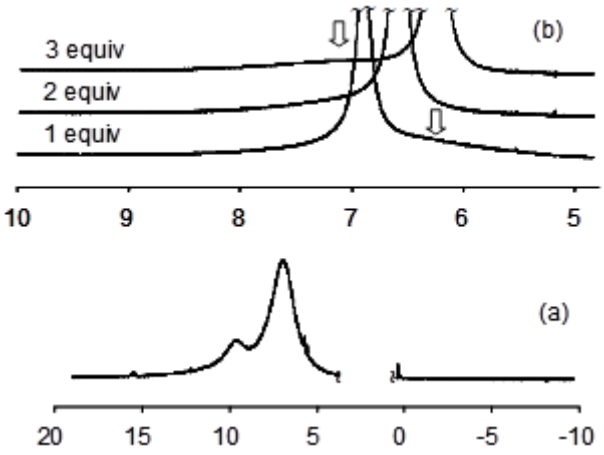

Figure 3. ^{1}H NMR spectra of $Co(acac)_2$-NEt_3 mixtures in acetone-d_6: (a) before NEt_3 addition; (b) after the addition of 1-3 equivalents.

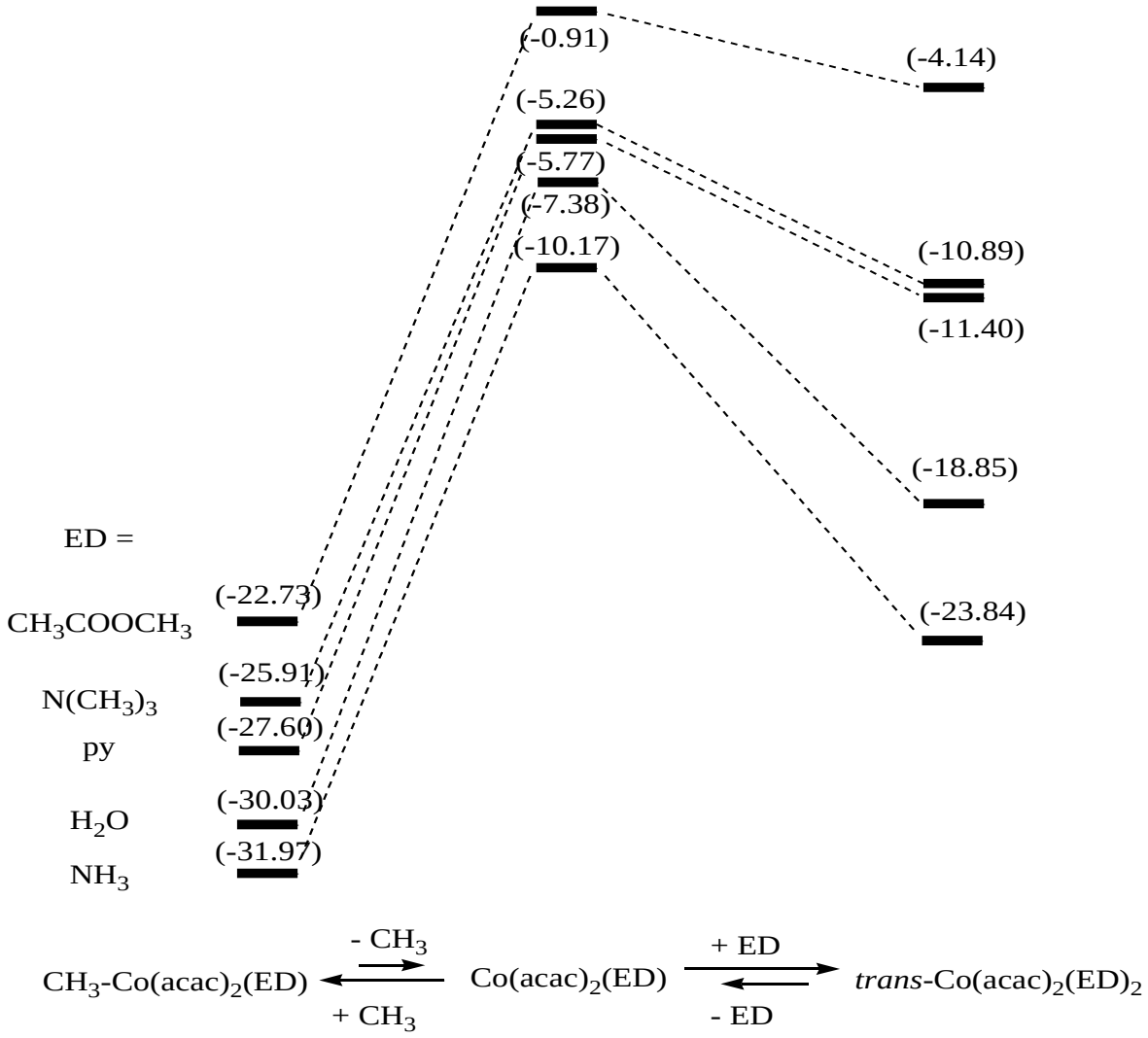

Figure 4. Relative DFT energies for model transformations of relevance to the controlled radical polymerization of VOAc.

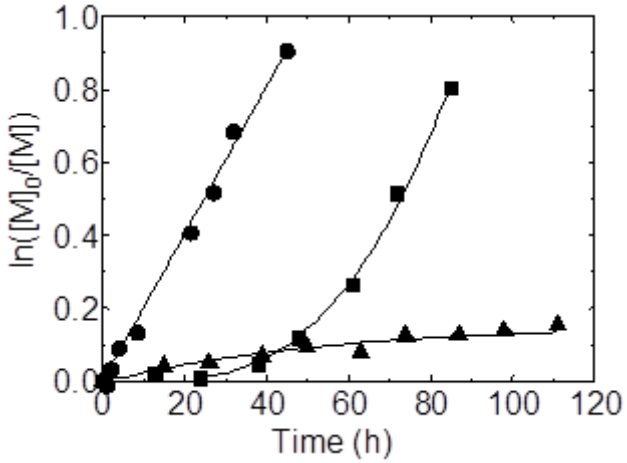

Figure 5. Semilogarithmic kinetic plots for the initial addition of electron donors (EDs) to bulk CRP of VOAc mediated by $Co(acac)_2$ with V-70 at 30 °C ($[VOAc]_0/[Co(acac)_2]_0/[V70]_0/[ED]_0$ = 500/1/1/30): (■) No addition, (●) Addition of py (30 equiv), (▲) Addition of NEt_3 (30 equiv).

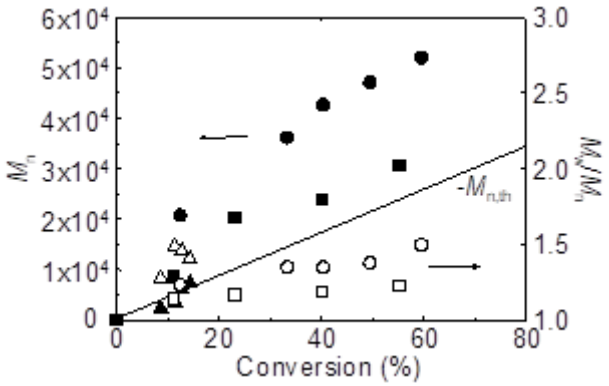

Figure 6. Evolution of M_n and M_w/M_n versus conversion for the initial addition of electron donors to bulk CRP of VOAc mediated by $Co(acac)_2$. Conditions are the same as in Figure 5. (■, □) No addition, (●, ○) Addition of py (30 equiv), (▲, Δ) Addition of NEt_3 (30 equiv).

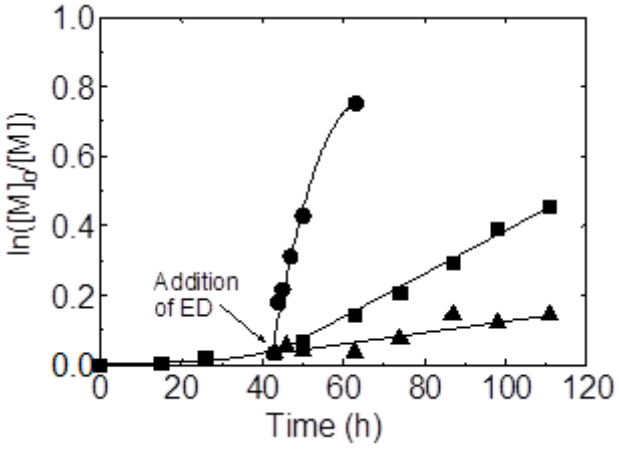

Figure 7. Semilogarithmic kinetic plots for the middle addition of electron donors to bulk CRP of VOAc mediated by $Co(acac)_2$. Conditions are the same as in Figure 5. (■) No addition, (●) Addition of py (30 equiv), (▲) Addition of NEt_3 (30 equiv).

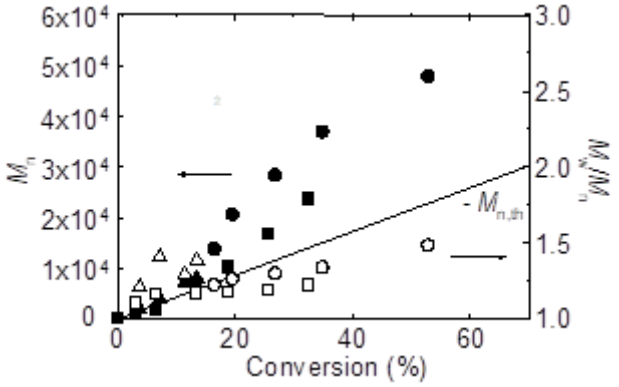

Figure 8. Evolution of M_n and M_w/M_n versus conversion for the late addition of electron donors to bulk CRP of VOAc mediated by $Co(acac)_2$. Conditions are the same as in Figure 5. (■, □) No addition, (●, ○) Addition of py (30 equiv), (▲, Δ) Addition of NEt_3 (30 equiv).

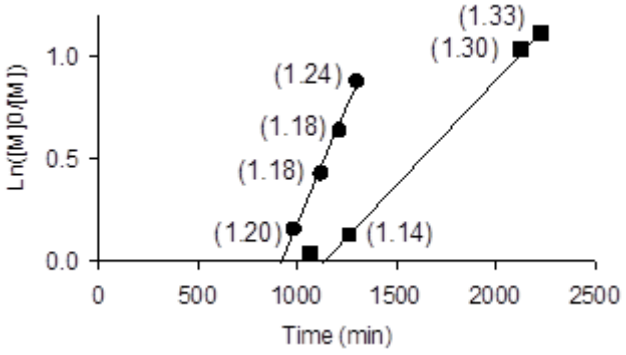

Figure 9. Semilogarithmic kinetic plots for the bulk CRP of VOAc mediated by $Co(acac)_2$ in the presence of different amounts of V-70 at 30 °C ($[VOAc]_0/[Co(acac)_2]_0/[ED]_0$ = 500/1/30): (■) $[V\text{-}70]_0/[Co(acac)_2]_0$ = 2; (●)$[V\text{-}70]_0/[Co(acac)_2]_0$ = 4. The values in parentheses indicate the polydispersity index of the polymer samples.

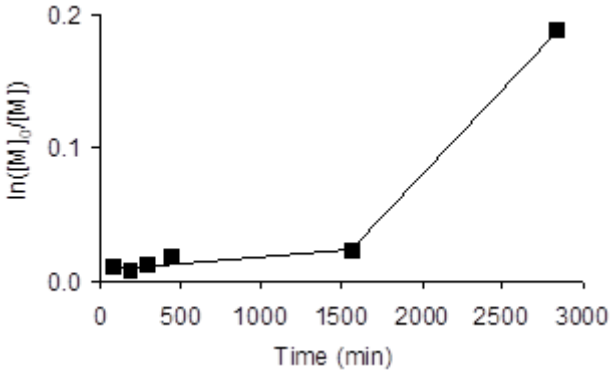

Figure 10. Semilogarithmic kinetic plots for the bulk CRP of VOAc mediated by pink $R_0(VOAc)_n$-$Co(acac)_2$ (M_n = 18800) at 40 °C ($[VOAc]_0/[Co^{III}]_0$ = 5400/1). Water ($[H_2O]/[Co^{III}]_0$= ca. 32) was added after 1566 min.

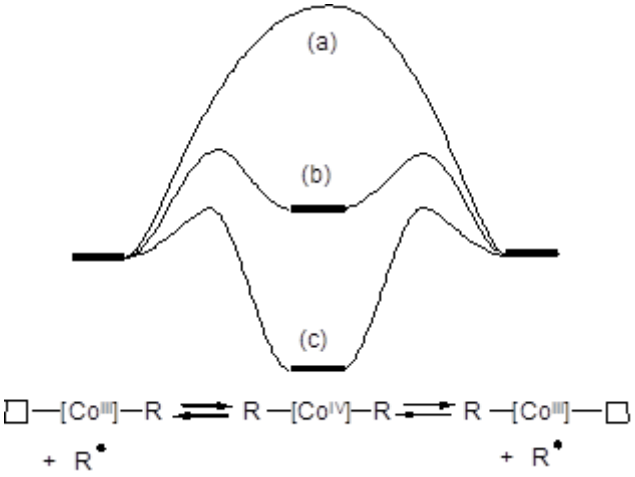

Figure 11. Possible energy profiles for the associative radical exchange on $(acac)_2Co^{III}$-PVOAc.

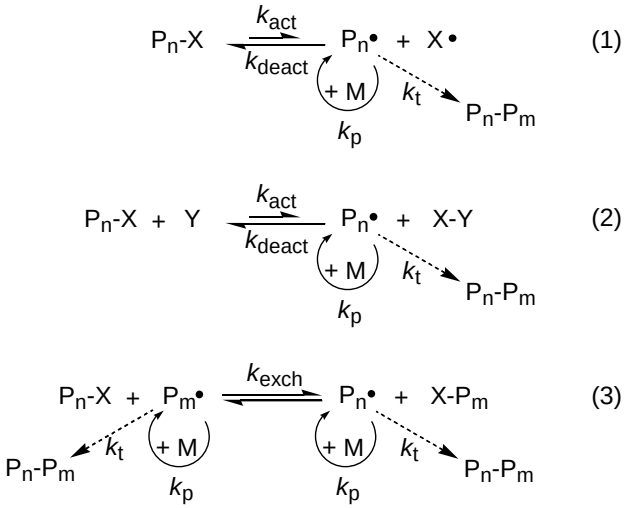

Scheme 1. General Mechanisms for Three Controlled/"Living" Radical Polymerizations.

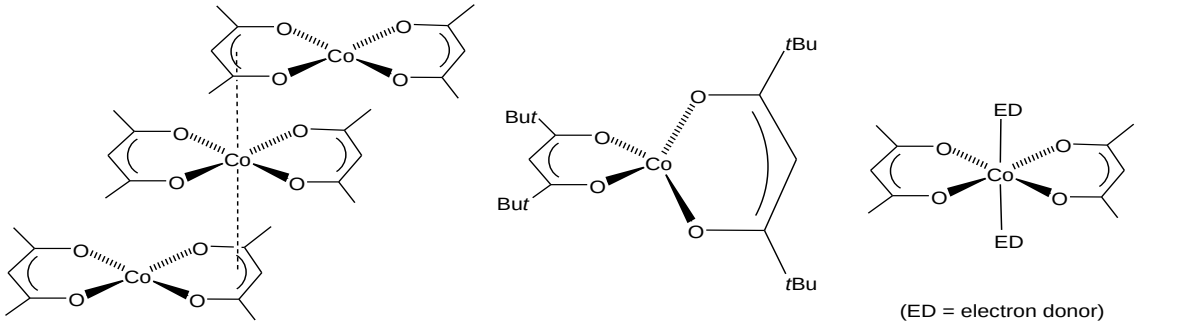

Sc

Scheme 2. Schematic representations of the molecular structures found for $[Co(acac)_2]$,[13] $[Co\{tBuC(O)CHC(O)tBu\}_2]$,[14a, 33] and $[Co(acac)_2(ED)_2]$.

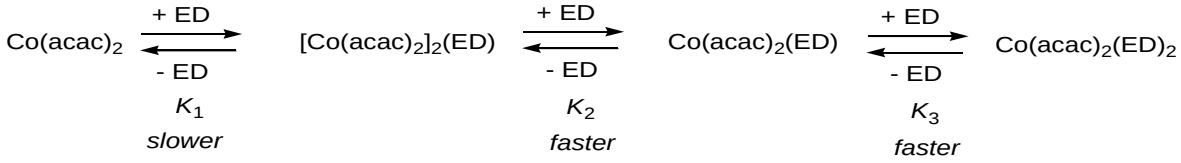

Scheme 3. Mechanism of ligand (ED) addition and exchange on $[Co(acac)_2]$.

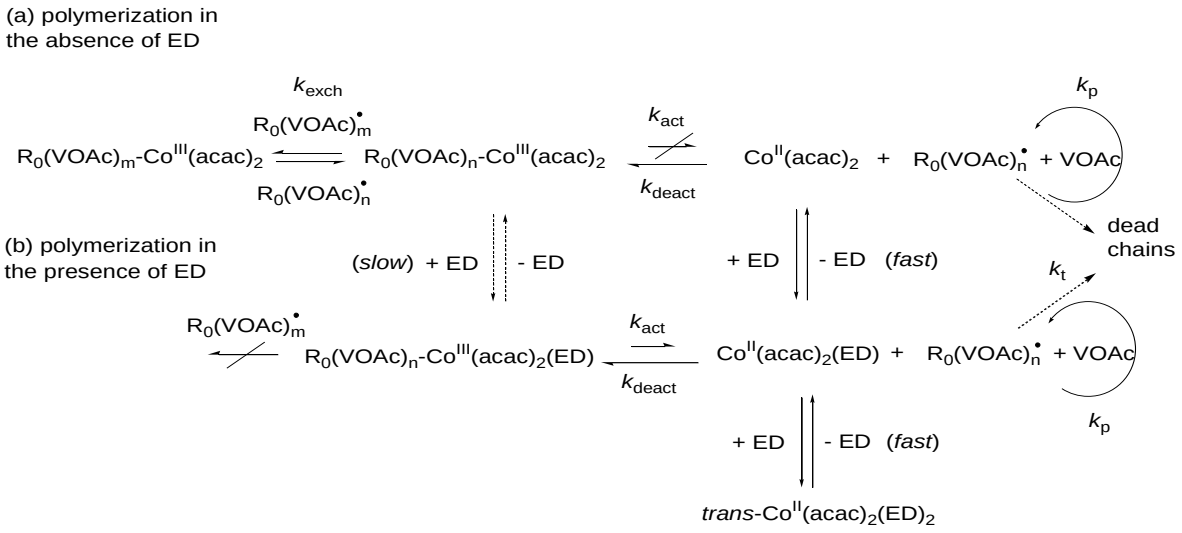

Scheme 4. Proposed General Mechanism for the CRP of VOAc Mediated by $Co(acac)_2$ Complex in the Absence and Presence of Electron Donors.

Table 1. DFT-optimized energies (in kcal mol^{-1}) of $Co(acac)_2(ED)_n$ (n = 0, 1, 2), relative to $[Co(acac)_2 + n(ED)]$.

n	ED	Geometry[a]	S	E
0	-	*tet*	3/2	0
	-	*sp*	1/2	8.80
1	CH_3COOCH_3	*tbp*	3/2	-0.91
	$N(CH_3)_3$	*tbp*	3/2	-5.26
	py	*tbp*	3/2	-5.77
	H_2O	*tbp*	3/2	-7.38
	H_2O	*spy*	3/2	-3.77
	NH_3	*tbp*	3/2	-10.17
2	CH_3COOCH_3	*oct*	3/2	-5.40
	$N(CH_3)_3$	*oct*	3/2	-10.89
	py	*oct*	3/2	-11.40
	H_2O	*oct*	3/2	-18.85
	NH_3	*oct*	3/2	-23.84

[a] *tet* = tetrahedral; *sp* = square planar; *tbp* = trigonal bipyramidal; *spy* = square pyramidal; *oct* = octahedral.

Table 2. DFT-optimized energies (in kcal mol^{-1}) of CH_3-$Co(acac)_2(ED)_n$ (n = 0, 1), relative to $[Co(acac)_2 + CH_3 + n(ED)]$.

n	ED	Geometry[a]	S	E
0	-	*sp*	0	-18.50
	-	*tbp*	1	-6.52
1	CH_3COOCH_3	*oct*	0	-22.73
	$N(CH_3)_3$	*oct*	0	-25.91
	py	*oct*	0	-27.60
	H_2O	*oct*	0	-30.03
	NH_3	*oct*	0	-31.97

Table of Context text

A new interplay between different mechanisms in controlled radical polymerization is revealed by a study of V-70 initiated vinyl acetate polymerization in the presence of $Co(acac)_2$. Coordination of the cobalt center by neutral electron donors switches the process from a degenerative transfer (DT), featuring an associative radical exchange, to an organometallic radical polymerization (OMRP), featuring a dissociative equilibrium for the Co^{III}-terminated dormant chain.

Table of Contents Graphic.

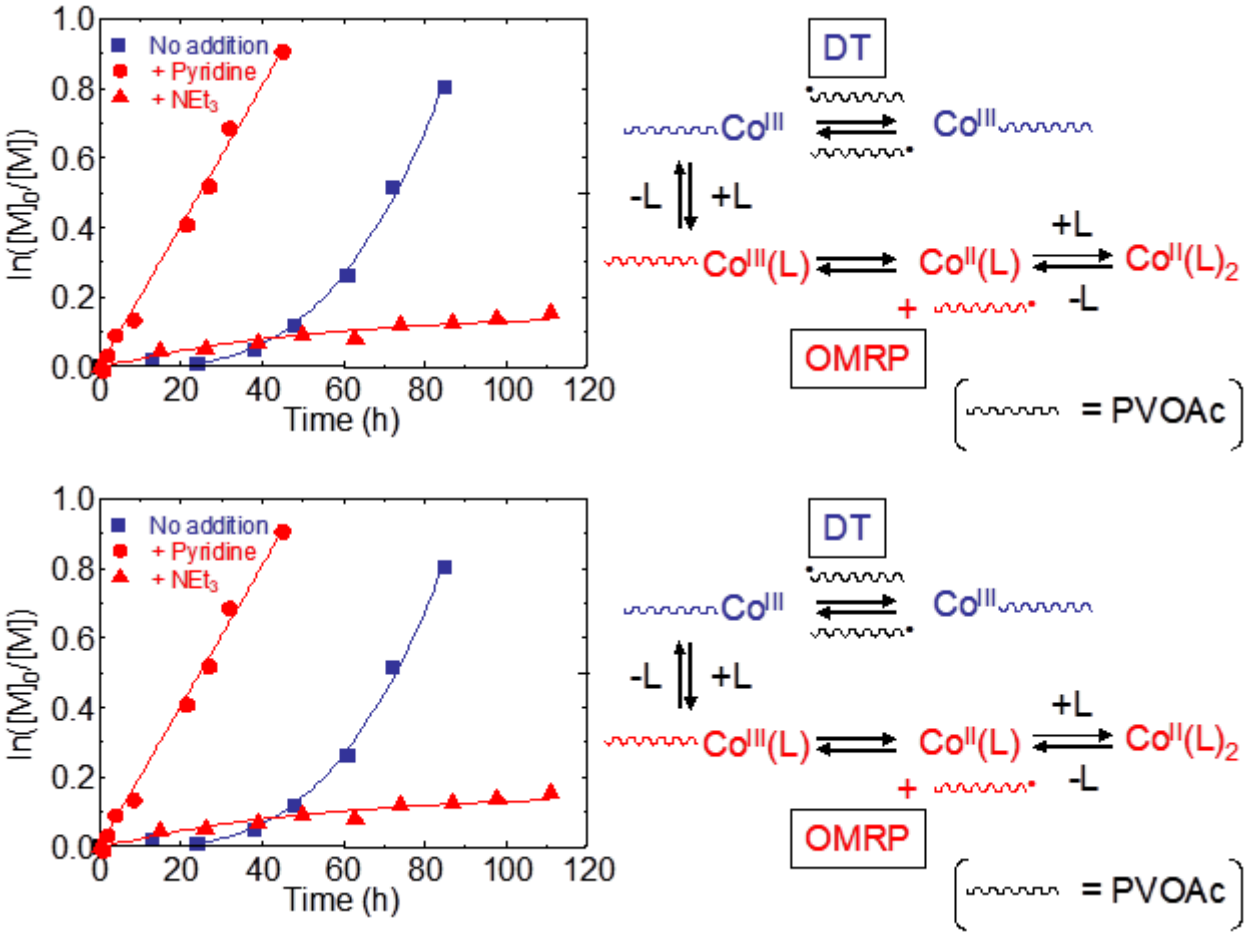

No addition
+ Pyridine
+ NEt3
ln([M]0/[M])
Time (h)
DT
CoIII
-L
+L
CoIII(L)
CoII(L)
CoII(L)2
OMRP
= PVOAc